High Energy Density Physics 17 (2015) 38–41

Contents lists available at ScienceDirect

High Energy Density Physics

journal homepage: www.elsevier.com/locate/hedp

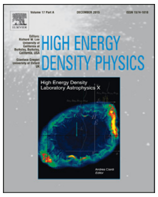

Numerical simulation of an experimental analogue of a planetary magnetosphere

Andy Sha Liao [a,*], Shule Li [b], Patrick Hartigan [a], Peter Graham [c], Gennady Fiksel [b], Adam Frank [b], John Foster [c], Carolyn Kuranz [d]

[a] Rice University, 6100 Main St., Houston, TX 77005, USA
[b] University of Rochester, 500 Joseph C. Wilson Blvd., Rochester, NY 14627, USA
[c] Awe PLC, Aldermaston, Reading, Berkshire RG7 4PR, United Kingdom
[d] University of Michigan, 500 S. State St., Ann Arbor, MI 48109, USA

ARTICLE INFO

Article history:
Available online 28 September 2014

Keywords:
Omega laser facility
MIFEDS
Laser astrophysics
Planetary magnetospheres
MHD
Methods: numerical

ABSTRACT

Recent improvements to the Omega Laser Facility's magneto-inertial fusion electrical discharge system (MIFEDS) have made it possible to generate strong enough magnetic fields in the laboratory to begin to address the physics of magnetized astrophysical flows. Here, we adapt the MHD code AstroBEAR to create 2D numerical models of an experimental analogue of a planetary magnetosphere. We track the secular evolution of the magnetosphere analogue and we show that the magnetospheric components such as the magnetopause, magnetosheath, and bow shock, should all be observable in experimental optical band thermal bremsstrahlung emissivity maps, assuming equilibrium charge state distributions of the plasma. When the magnetosphere analogue nears the steady state, the mid-plane altitude of the magnetopause from the wire surface scales as the one-half power of the ratio of the magnetic pressure at the surface of the free wire to the ram pressure of an unobstructed wind; the mid-plane thickness of the magnetosheath is directly related to the radius of the magnetopause. This behavior conforms to Chapman and Ferraro's theory of planetary magnetospheres. Although the radial dependence of the magnetic field strength differs between the case of a current-carrying wire and a typical planetary object, the major morphological features that develop when a supersonic flow passes either system are identical. Hence, this experimental concept is an attractive one for studying the dynamics of planetary magnetospheres in a controlled environment.

1. Introduction

The magnetic force, and hence magnetic pressure, contributes significantly to the dynamics that govern many astrophysical phenomena including accretion columns feeding young stars [1], starspots [2], flows of gas in stellar coronae [3–6], and the space environment near magnetized planets [7–10]. The magnetic field plays a key role in these objects by constraining the cross-field motion of the plasma inside the magnetized region, and as a medium of energy storage and transport. In the case of magnetized accretion columns, simulations show that when the magnetic pressure is a significant contributor to the total pressure of the gas within the column, splashing of the accreting material as it impacts the stellar surface was greatly reduced from that observed in the case of a non-magnetized accretion column [1]. On stellar photospheres, including that of the Sun, the increased magnetic pressure in the vicinity of bunched magnetic flux tubes can impede the normal transport of energy from the stellar interior. This produces cooler and darker regions on the stars' surface observable as starspots [2]. Additionally, observations and MHD simulations demonstrate that stellar coronae are given their global appearance by the stellar magnetic field that binds and directs the flows of plasma. Sudden relaxations of the magnetic constraints, particularly by magnetic reconnections can produce energetic events including flares and coronal mass ejections (CMEs) [3,4,6]. Finally, strong magnetic fields generated by a planetary dynamo deflect the solar wind high above the planet's surface. The interaction between the planetary magnetic field and the solar wind produces the structures of the planet's magnetosphere [7,8].

---

[*] Corresponding author.
E-mail address: Andy.Liao@rice.edu (A.S. Liao).

http://dx.doi.org/10.1016/j.hedp.2014.09.005
1574-1818/

Chapman and Ferraro [7,11–15] developed the first modern theory of planetary magnetospheres in the 1930's. In their model, the edge of the solar wind forms a conducting surface in its approach towards a magnetized planet. When the wind plasma deflects around the planet's magnetic field, the magnetic field anchored to the planetary dynamo reacts through a compression on its windward side, and a rarefaction into a long tail on its leeward side. The solar wind compresses the planetary field by the same amount as would occur from the superposition of an image magnetic dipole upon the original planetary field, where the source of the image dipole is located upstream from the wind stagnation point by a distance equal to that of the downstream separation of the planet from the stagnation point. As the wind deflects around the planet and its magnetic field, the wind's inner edge settles where the magnetic pressure and the wind's ram pressure balances, and forms the planet's magnetopause. When the supersonic solar wind encounters a magnetized planet, the magnetopause acts as the effective surface of the planet-as-obstacle. A bow shock [16–19] forms at the location as expected when the supersonic wind encounters a non-magnetized planet with a radius equal to that of the magnetopause around a magnetized planet.

However, real magnetospheres are neither static, nor are they as simple as modeled in Chapman and Ferraro's theory. For example, terrestrial magnetic storms arise due to the time variations in the direction of the magnetic field embedded in the solar wind stream. Variations in the solar wind density and velocity also affect the magnetosphere. Given the complexities of real magnetospheres, it is desirable to develop a platform to study the phenomena in a controlled laboratory environment. Any laser experimental platform that replicates the basic physics of planetary magnetospheres may be extended to explore more complex magnetospheric phenomena such as storms. To date, laser experiments have not successfully reproduced the global properties of a magnetosphere because highly magnetized supersonic flows are a new frontier in high-energy-density laboratory techniques [20].

In this paper, we discuss a new laser experimental concept to reproduce the behaviors and structures seen in a steady-state planetary magnetosphere. We describe the experimental design and our models in Section 2, and in Section 3 we show the results of our numerical simulations. In Section 4 we discuss the overall feasibility of realizing the experiment and compare our results with predictions from the Chapman–Ferraro theory.

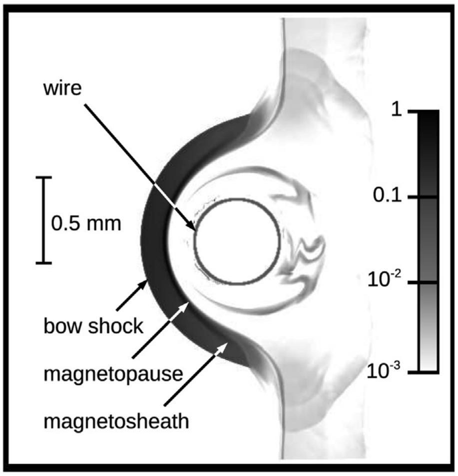

Fig. 1. Normalized logarithmic-scaled free–free emissivity map was created from a snapshot at 3.9 wire-crossing times for a simulation with a magnetized wire. Because of the magnetic field surrounding the wire, the wind was deflected roughly 100 μm above wire's surface marked by the circle. The emission source region, having detached from the wire, forms the magnetosheath. The magnetosheath is bound by a bow shock on its windward side and a magnetopause on its leeward side. The arrangement seen here replicates the structure of a planetary magnetosphere.

2. Model

2.1. Wire concept

A relatively simple way to test the Chapman–Ferraro law is to employ a straight current-carrying wire as the analogue to the planetary magnetic field. The main disadvantages that arise from this scheme are geometric in origin: The wire-as-obstacle-in-flow is cylindrical, not spherical like a planet the real solar wind encounters. The magnetic field that is generated by a straight wire is also cylindrical, and its strength falls off with distance R from the wire axis with R^{-1}, again deviating from the astrophysical scenario of a planetary dipole field that falls off with distance with R^{-3}. In spite of the differences between our scheme and the astrophysical scenario, the Chapman–Ferraro law holds regardless of the particular geometry of the magnetic field, and remains testable in our model as long as the magnetic field is strong enough to deflect the wind at a visibly higher altitude from the wire surface than what is expected when the wind encounters a nonmagnetized wire.

2.2. Wire simulations

Our numerical models were completed using AstroBEAR, an AMR radiation and magneto-hydrodynamics code developed at the University of Rochester [21]. In our AstroBEAR simulations, a 2D grid of 501 by 501 cells, or in physical dimensions a square of 2.5 mm was initialized. First, an infinitely-long wire object of 250 μm radius was inserted into the center of the grid square in cross-section. An ambient medium took the place of the remaining space on the grid. A magnetic field was imposed, ad-hoc, in the space surrounding the wire to simulate a current flowing through the wire. The vector potential of the imposed magnetic field was

$$A = (20\ \mathrm{T})(250\ \mu\mathrm{m})\ln\left(\frac{R}{250\ \mu\mathrm{m}}\right)\hat{z} \tag{1}$$

where R for $R > 250\ \mu\mathrm{m}$ is the radial distance from the wire axis and the grid spans the xy plane. Finally, a wind object was initialized to supply a constant, uniform flux of material from one edge of the grid during runtime.

The ratio of initial densities of ambient medium, wind and wire was maintained to be $3{:}40{:}3 \times 10^5$ throughout this series of simulations even as the density and velocity of the wind was changed from run to run in order to explore the parameter space. The temperature of the wind and ambient medium was maintained across all simulations to be 300 K; the temperature of the wire was taken to be 3 mK to maintain pressure equilibrium between the wire and ambient medium.

The equation of state of all components was taken to be that of the ideal gas and the MHD calculations were nonresistive for neutral plasmas. Evolution was tracked up to 5.3 wire-crossing times, i.e. the time it takes for the wind at onset to cross 500 μm down range, the wire diameter. Snapshots for further processing were taken at 3.9 wire-crossing times.

2.3. Post-processing

In order to simulate the data produced by the Gated Optical Imager (GOI) [22] at the Omega Laser Facility, maps of free–free emissivity in the optical band between 400 nm and 700 nm